frontiers in Physics

ORIGINAL RESEARCH
published: 22 November 2018
doi: 10.3389/fphy.2018.00127

Confronting SUSY GUT With Dark Matter, Sparticle Spectroscopy and Muon $(g-2)$

Mario E. Gómez[1]*, Smaragda Lola[2,3], Roberto Ruiz de Austri[4] and Qaisar Shafi[5]

[1] Departamento de Ciencias Integradas, Facultad de Ciencias Experimentales, Universidad de Huelva, Huelva, Spain, [2] Institute of Nuclear and Particle Physics, NCSR "Demokritos," Athens, Greece, [3] Department of Physics, University of Patras, Patras, Greece, [4] Instituto de Física Corpuscular, IFIC-UV/CSIC, Valencia, Spain, [5] Department of Physics and Astronomy, Bartol Research Institute, University of Delaware, Newark, DE, United States

We explore the implications of LHC and cold dark matter searches for supersymmetric particle mass spectra in two different grand unified models with left-right symmetry, $SO(10)$ and $SU(4)_c \times SU(2)_L \times SU(2)_R$ (4-2-2). We identify characteristic differences between the two scenarios, which imply distinct correlations between experimental measurements and the particular structure of the GUT group. The gauge structure of 4-2-2 enhances significantly the allowed parameter space as compared to $SO(10)$, giving rise to a variety of coannihilation scenarios compatible with the LHC data, LSP dark matter and the ongoing muon g-2 experiment.

Keywords: grand unification, supersymmetry, dark matter, LHC, sparticle spectroscopy

OPEN ACCESS

Edited by:
Theocharis S. Kosmas, University of Ioannina, Greece

Reviewed by:
Suchita Kulkarni, Institute of High Energy Physics (OAW), Austria
Michael Andreas Schmidt, University of New South Wales, Australia

****Correspondence:***
Mario E. Gómez
mario.gomez@dfa.uhu.es

Specialty section:
This article was submitted to High-Energy and Astroparticle Physics, a section of the journal Frontiers in Physics

Received: *29 June 2018*
Accepted: *19 October 2018*
Published: *22 November 2018*

Citation:
Gómez ME, Lola S, Ruiz de Austri R and Shafi Q (2018) Confronting SUSY GUT With Dark Matter, Sparticle Spectroscopy and Muon (g − 2). Front. Phys. 6:127. doi: 10.3389/fphy.2018.00127

1. INTRODUCTION

In recent years, LHC results [1, 2][1,2] and dark matter searches [3–8][3] severely constrain some of the simplest standard model (SM) extensions. Nevertheless, we know that we have to find a way to go beyond the standard theory, which cannot accommodate massive neutrinos, nor explain the observed baryon asymmetry of the universe and recent cosmological observations [9–12]. These issues can be addressed by imposing further unification, including grand unified theories and supersymmetry, which among others provides a natural candidate for dark matter [13, 14].

Here we consider two supersymmetric models with gauge unification at M_{GUT}, $SO(10)$ [15, 16] and $SU(4)_c \times SU(2)_L \times SU(2)_R$ (4-2-2) [17–24]. We assume that at that scale the SUSY soft terms still preserve the group symmetry. This idea has been implemented in previous work for several GUTs [25–33]. Here, we focus on the effects derived from the gauge structure of the two groups, while the sfermion mass terms remain universal, with all matter being contained in a single representation of the gauge group[4]. However, the soft higgs masses differ, since this sector is contained in different representations. The main difference between the two groups arises in the gaugino sector: for $SO(10)$ it is natural to assume gauge mass universality, since this symmetry is broken to SM at the GUT scale. In the case of 4-2-2, however, the SM gauge couplings arise from combining broken and unbroken symmetries of the group, allowing different GUT relations among the gaugino masses.

[1]For a compendium of CMS searches for supersymmetry, see https://twiki.cern.ch/twiki/bin/view/CMSPublic/PhysicsResultsSUS
[2]For a compendium of ATLAS searches for supersymmetry, see https://twiki.cern.ch/twiki/bin/view/AtlasPublic/SupersymmetryPublicResults
[3]http://www.xenon1t.org/
[4]This is the case in SO(10), but also in the LR symmetric 4-2-2. A larger study relaxing the LR symmetry in the 4-2-2 case is presented in Gomez et al. [34].

Even though the two models differ in just a single relation for the gaugino masses, this results to vastly different phenomenological predictions. Among others, the possibility of small LSP masses in 4-2-2 enables satisfying the relic density predictions due to coannihilations, and gives rise to direct detection cross sections in the range of the current experiments, as well as visible signals at the LHC. It is also interesting to investigate whether in any of the two groups the discrepancy between the experimental value of the anomalous magnetic moment of the muon and the SM prediction [35], can be explained through supersymmetric contributions.

Within this framework, we study the predictions for sparticle spectroscopy in the two scenarios, also requiring LSP dark matter through coannihilations. We identify distinct differences between the two groups, which result in direct correlations between the experimental measurements and the group structure and symmetries, which can be tested in future searches.

2. GUT MODELS AND INPUT PARAMETERS

As in [25], where $SO(10)$ has been compared with $SU(5)$ and flipped $SU(5)$, we assume that SUSY breaking occurs at a scale $M_X > M_{GUT}$, through a mechanism that generates flavor blind soft-terms. Between the scales M_X and M_{GUT}, renormalization and additional flavor symmetries may induce non-universalities for soft terms that belong to different representations; on the contrary, particles that belong to the same representation have common soft masses.

The soft terms for the fields in an irreducible representation r of the unification group are defined as multiples of a common scale m_0 as:

$$m_r = x_r\, m_0, \tag{1}$$

while the trilinear terms are defined as:

$$A_r = Y_r\, A_0, \quad A_0 = a_0\, m_0. \tag{2}$$

Here, Y_r is the Yukawa coupling associated with the r representation. We use the standard parametrisation, with a_0 being a dimensionless factor, which we consider as representation-independent. This is justified because the representation dependence is already taken into account in the Yukawa couplings, and including a further factor can be confusing.

Let us see how the above are applicable to the two gauge groups under discussion:

• *SO*(10)

The simplest possibility arises within an $SO(10)$ GUT, in which all quarks and leptons are accommodated in the same **16** representation, leading to left-right symmetric mass matrices. We assume that the up and down higgs fields are in a pair of **10** representations. This assignment determines sfermion mass matrices and beta functions, and results in a common mass for all sfermions and two different higgs masses m_{h_u} and m_{h_d} (thus identified with the NUHMSSM).

In addition to the CMSSM, therefore, we introduce two new parameters x_u and x_d defined as:

$$m_{16} = m_0, \quad m_{H_u} = x_u\, m_{16}, \quad m_{H_d} = x_d\, m_{16}. \tag{3}$$

Similarly, the A-terms are defined as:

$$A_{16} = a_0 \cdot m_0. \tag{4}$$

• 4-2-2

The main features of the 4-2-2 that are relevant for our discussion are summarized below. The 4-2-2 gauge symmetry can be obtained from a spontaneous breaking of SO(10) by utilizing either the 54 dimensional or the 210 dimensional representation, allowing for some freedom of choice. The former case, where $SO(10)$ breaks through a Higgs 54-plet can be naturally combined with a left-right symmetry [34]. By contrast, this left-right symmetry is explicitly broken in the latter case. Here, we will mostly focus on the left-right symmetric 4-2-2 model, which has the minimal number of free parameters and can be more directly compared with $SO(10)$. In this case, the gaugino masses associated with $SU(2)_L$ and $SU(2)_R$ are the same, while the gluino mass, associated with $SU(4)_c$, can differ.

The main relations are therefore the following:

- Gaugino masses: The hypercharge generator from 4-2-2 implies the relation

$$M_1 = \frac{3}{5}M_2 + \frac{2}{5}M_3. \tag{5}$$

- Soft masses: All sfermions are accommodated in a 16 representation, and have a common mass $m_{16} = m_0$. The Higgs fields are in a 10-dimensional representation with D-term contributions that result to $m^2_{H_{u,d}} = m^2_{10} \pm 2M^2_D$. In our notation, these values are:

$$r_u = \frac{m_{H_u}}{m_{16}}; \qquad r_d = \frac{m_{H_d}}{m_{16}}; \tag{6}$$

  with $r_u < r_d$.

For both models we start our analysis at the GUT scale, assuming the particle content of the MSSM with a pattern of soft masses determined by the corresponding unification symmetry. At low energies, this results in sparticle mass relations that can be manifest in phenomenological predictions (DM or LHC signals), thus providing information on the specific GUT symmetry. In our computations we assume a common unification scale M_{GUT} defined as the meeting point of the g_1 and g_2 gauge couplings. The GUT value for g_3 is obtained by requiring $\alpha_s(M_Z) = 0.187$. Above M_{GUT} we assume a unification group that breaks at this scale. SUSY is broken above M_{GUT} by soft terms that are representation-dependent while preserving flavor blindness. We integrate the RGE's by using *SoftSusy* [36], such that all the analyzed models are consistent with electroweak symmetry breaking. We perform a parameter space scan using as a guide the representation pattern at the GUT scale for soft scalar terms. For this purpose, we extend the CMSSM universal scenario through non-unified soft terms, consistent with the representations of SO(10) and 4-2-2. Even in their simplest versions, these scenarios result in soft term correlations that enlarge the size of the parameter space that is compatible with the neutralino relic density from Planck. Note that the charge and color breaking minima constraints are not taken into account; however, they may be present at some points, especially the ones with stau or stop coannihilations [37, 38].

We perform runs with soft terms up to 10 TeV and a parameter range summarized below:

$$\begin{aligned}
100\text{GeV} \le &\quad m_0 \quad \le 10\text{TeV}\\
50\text{GeV} \le &\quad M_1 \quad \le 4\text{TeV}\\
50\text{GeV} \le &\quad M_2 \quad \le 4\text{TeV}\\
-10\text{TeV} \le &\quad A_0 \quad \le 10\text{TeV}\\
2 \le &\; \tan\beta \; \le 65\\
-1.9 \le &\quad x_u \quad \le 1.5\\
0 \le &\quad x_d \quad \le 3.4\\
x_u &\quad \le \quad x_d
\end{aligned} \tag{7}$$

3. EXPERIMENTAL CONSTRAINTS AND PARAMETER SPACE SCAN

For our analysis we use Superbayes [39–41], a package that includes MSSM RGEs [36] , DM computations [42, 43], phenomenological bounds and updated LHC bounds on SUSY particles, as well as phenomenological constraints derived from b-physics [44, 45]. We further impose the constraint on the neutralino-nucleon cross section provided by the more recent Xenon-100 and LUX upper limits [46]. SuperBayeS-v2.0 runs a sample algorithm using the code MultiNest v2.18 [47, 48]. Superbayes offers the possibility to cover a much larger sector of the parameter space than a simple random search, since it uses a likelihood function that orients the sampling toward regions that fit the experimental data (see [25, 34] for details). We performed two scans of the parameter space: the first uses logarithmic priors, appropriate for exploring large areas of the parameter space, and for finding points that satisfy the relic density constraint due to $\tilde{\chi}^0$ annihilations; the second one uses flat priors, which are efficient for identifying the parameter correlations required to satisfy the previous constraint due the coannihilations of $\tilde{\chi}^0$ with other particles. The results are presented by combining the two searches. A further statistical analysis would have required a much larger sampling, and is beyond the scope of this work.

It is well known that, if the required amount of relic dark matter is provided by neutralinos, particular mass relations must be present in the supersymmetric spectrum. In addition to mass relations, we use the neutralino composition to classify the relevant points of the supersymmetric parameter space. The higgsino fraction of the lightest neutralino mass eigenstate is characterized by the quantity

$$h_f \equiv |N_{13}|^2 + |N_{14}|^2 , \tag{8}$$

where the N_{ij} are the elements of the unitary mixing matrix that correspond to the higgsino mass states. Thus, we classify the points that pass the constraints discussed in section 2 according to the following criteria:

- **Higgsino $\tilde{\chi}^0$:**

$$h_f > 0.1, \quad |m_A - 2m_{\tilde{\chi}|^0} > 0.1\, m_{\tilde{\chi}^0}. \tag{9}$$

  In this case, the lightest neutralino is higgsino-like and, as we discuss later, the lightest chargino $\tilde{\chi}_1^{\pm}$ is almost degenerate in mass with the $\tilde{\chi}^0$. The couplings to the SM gauge bosons are not suppressed and $\tilde{\chi}^0$ pairs have large cross sections for annihilation into W^+W^- and ZZ pairs, which may reproduce the observed value of the relic abundance. Clearly, coannihilation channels involving $\tilde{\chi}_1^{\pm}$ and $\tilde{\chi}_2^0$ also contribute.
- ***A*/*H* resonances:**

$$|m_A - 2m_{\tilde{\chi}^0}| \le 0.1\, m_{\tilde{\chi}^0}. \tag{10}$$

  The correct value of the relic abundance is achieved thanks to *s*-channel annihilation, enhanced by the resonant *A* propagator. The thermal average $\langle \sigma_{ann} v \rangle$ spreads out the peak in the cross section, so that neutralino masses for which $2m_{\tilde{\chi}^0} \simeq m_A$ does not exactly hold, can also undergo resonant annihilations.
- **$\tilde{\tau}$ coannihilations:**

$$h_f < 0.1, \quad (m_{\tilde{\tau}_1} - m_{\tilde{\chi}^0}) \le 0.1\, m_{\tilde{\chi}^0} \tag{11}$$

  The neutralino is bino-like, annihilation into leptons through *t*-channel slepton exchange is suppressed, and coannihilations involving the nearly-degenerate $\tilde{\tau}_1$ are necessary to enhance the thermal-averaged effective cross section.

In the 4-2-2 model we get three additional types of coannihilation:

- **$\tilde{\chi}^+$ coannihilations:**

$$h_f < 0.1, \quad (m_{\tilde{\chi}^+} - m_{\tilde{\chi}^0}) \le 0.1\, m_{\tilde{\chi}^0}. \tag{12}$$

  The lightest chargino is light and nearly degenerate with the bino-like neutralino.
- **$\tilde{g}$ coannihilations:**

$$h_f < 0.1, \quad (m_{\tilde{g}} - m_{\tilde{\chi}^0}) \le 0.1\, m_{\tilde{\chi}^0}. \tag{13}$$

  The gluino is light and nearly degenerate with the bino-like neutralino.
- **$\tilde{t}_1$ coannihilations:**

$$h_f < 0.1, \quad (m_{\tilde{t}_1} - m_{\tilde{\chi}^0}) \le 0.1\, m_{\tilde{\chi}^0}. \tag{14}$$

  The $\tilde{t}_1$ is light and nearly degenerate with the bino-like neutralino. These coannihilations were found to also be present in the flipped SU(5) model (but not *SO*(10) or *SU*(5)).

The higgsino mass ratios have been chosen so that we have minimal overlapping among the different classes of points. We note that the LR symmetry in the scalar soft masses does not allow scenarios with $\tilde{\nu} - \tilde{\tau} - \tilde{\chi}^0$ coannihilations, which appear in the SU(5) scenarios of Cannoni et al. [25] or in the LR asymmetric 4-2-2.

4. PLANCK COMPATIBLE REGIONS, MUON ANOMALOUS MAGNETIC DIPOLAR MOMENT AND DARK MATTER SEARCHES

In $SO(10)$, the DM regions compatible with the Planck neutralino relic density are similar to the CMSSM. However, their parameter space is enlarged due to the two independent higgs mass terms (essentially reproducing the non-universal Higgs CMSSM). Due to the additional freedom, $\tilde{\tau} - \chi$ coannihilations (orange circles in the figures) correspond to neutralino masses below 650 GeV. Resonances of the pseudoscalar Higgs-mediated neutralino annihilation channels (brown crosses in the figs.) are present in the entire range of m_χ under consideration, to be contrasted to the funnel-like area of the CMSSM. Neutralinos with a large higgsino component are localized at values m_χ around 1 TeV.

In 4-2-2, the GUT relation among the Higgsino masses results to wino-like charginos and low mass gluinos that can coannihilate with the lightest neutralino. Moreover, even if the sfermion masses are kept universal at the GUT scale, it is possible to find models where light stops can coannihilate with the neutralino. In 4-2-2, therefore, the additional freedom among the GUT values of the gaugino masses introduces three new types of coannihilations that satisfy the Planck neutralino relic density requirements.

4.1. Muon g-2

The discrepancy between the experimental measurement of the muon $g-2$ and the respective SM prediction, $\delta a_\mu^{SUSY} = (28.7 \pm 8.2) \times 10^{-10}$, can be attributed to additional contributions from SUSY particles. However, for these contributions to be above the 3-σ level, sparticle masses below $\sim$ 500 GeV are required. By contrast, the experimental values for the Higgs mass [1, 2] can be accommodated in SUSY models with universal soft terms at the GUT scale with a heavy SUSY spectrum. Since in 4-2-2 unification the less restrictive gaugino mass relations allow a lighter SUSY spectrum than in SO(10) (also compatible with DM, especially for the models with chargino coannihilations), we expect that the study of δa_μ^{SUSY} favors this unification group.

In **Figure 1** we display the prediction for δa_μ^{SUSY} vs. the neutralino mass values. Although this will be discussed later we include, already at this stage, the points excluded by the LHC analysis. We can see that the value of δa_μ^{SUSY} is always lower than the central value. In the case of SO(10), we can see that just a few points can produce a significant contribution to the muon g-2 (however, these points are excluded by the LHC bounds). In the case of 4-2-2 however, several points are compatible with a contribution to the muon g-2; even though the respective region is small, it is compatible with chargino and stau coannihilation regions that are not excluded by the LHC bounds.

4.2. Dark Matter Searches

The relation among different soft-terms will determine the composition of the neutralino, which is important for its detection. In this respect, different GUTs result to different predictions, which can be tested in both direct and indirect detection experiments. Here, we compare the spin-independent (SI) neutralino-nucleon cross section of the models under consideration, with the experimental bounds and prospects. Although spin-dependent [8] and indirect detection bounds also exclude many SUSY models, the current and projected experiments for the SI neutralino-nucleon cross section can test the predictions of the majority of the models considered here.

Figure 2 is indicative of how a change in the gauge unification conditions results in a significant enhancement of the parameter space when passing from $SO(10)$ to 4-2-2. It is also possible to see how the direct detection bounds can impose important constraints on the parameter space. For instance, we can see that the latest update of the Xenon-1T bound[3] excludes many points with A-resonances and higgsino DM regions, especially in the case of the 4-2-2 model. Moreover, **Figure 2** shows that projected experiments can be sensitive to most of the parameter space presented here. In the case of SO(10), DARWIN will cover the entire parameter space. In the case of 4-2-2, certain areas of $\tilde{\chi}^\pm - \chi$ still remain below detection prospects.

5. LHC SEARCHES

In this section, we investigate the constraints imposed by the LHC on the unified SUSY models under consideration. Each model can be associated with a particular set of particle hierarchies and decays, which are then compared with the generic data provided by the ATLAS and CMS collaborations [49, 50]. These comparisons are made with the help of Simplified Model Spectra (SMS) which can be defined by a set of hypothetical SUSY particles and a sequence of products and decay modes that have to be compared with those expected in our specific model. As a result, an individual check has to be done for every model, while, due to mismatches between the theoretical and the experimental results, it is not possible to provide contour plots where one can easily see which mass ranges are excluded. This task is simplified by using public packages like *Smodels-v1.1.1.* [51], which provides a powerful tool to perform a fast analysis of a large number of models [52, 53]. By using this package, the theoretical models are decomposed in SMS and can be contrasted with the existing LHC bounds if there is a match in the respective topologies. The practical procedure departs from the particle mass spectrum computation with SoftSusy [36], which is used to compute decay branching ratios using SUSY-HIT [54]; production cross-sections are calculated by Smodels-v1.1.1 which calls Pythia 8.2 [55].

In **Figures 3–6** we classify the models as (i) the ones that can be compared with the LHC data (either satisfying the bounds or being excluded) and (ii) those that cannot be tested at the

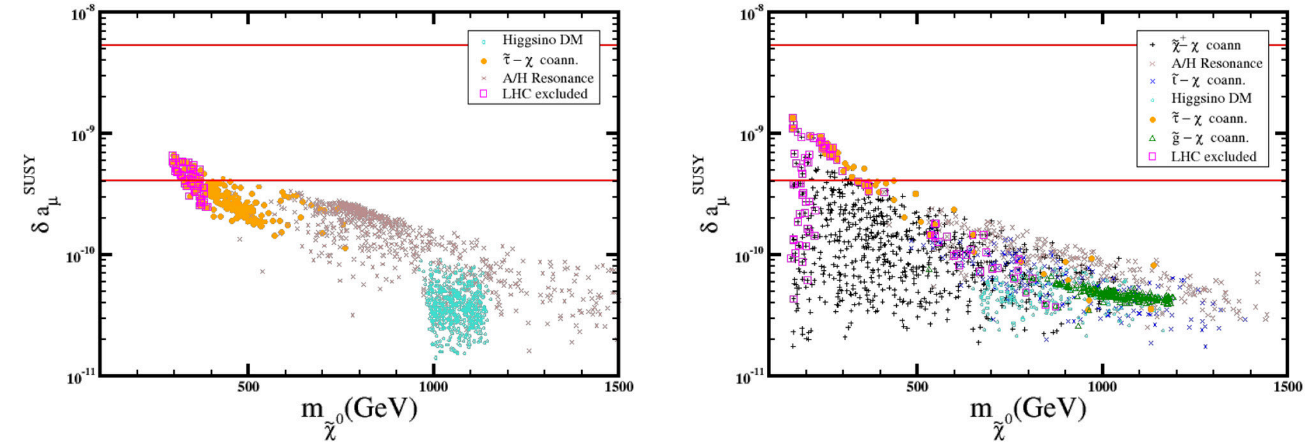

FIGURE 1 | Prediction for δa_μ^{SUSY} vs. m_χ. The red lines denote the 3-σ bounds for the experimental discrepancy of a_μ with respect to the SM prediction. The left plot corresponds to SO(10) and the right to 4-2-2. Different symbols and color codes are assigned to each class of models and this notation is maintained in the rest of the plots as well: Turquoise dots stand for Higgsino DM, black crosses for $\tilde{\chi}^\pm - \chi$ coannihilations, brown crosses for A/H resonances, blue crosses for $\tilde{t} - \tilde{\chi}^0$ coannihilations, orange dots for $\tilde{\tau} - \tilde{\chi}^0$ coannihilations, and green triangles for $\tilde{g} - \tilde{\chi}^0$ coannihilations.

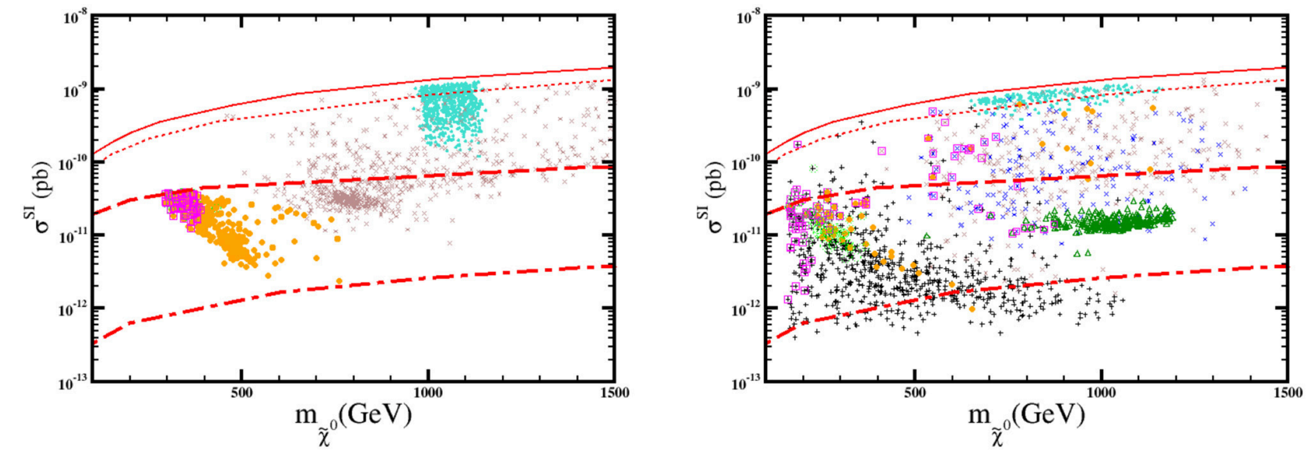

FIGURE 2 | Scatter plots for the SI neutralino-nucleon cross section, for SO(10) (left) and 4-2-2 (right). The red line corresponds to the Xenon-1T bound [6] while the dotted line includes their latest announcement. The dash and the dot-dash lines correspond to the projected sensitivities from LZ [4] and DARWIN [7]. Symbols and color codes are the same as in **Figure 1**.

LHC; the later are points that either predict processes with very low cross sections or result in topologies that are not tested at the LHC. For the points of category (i), we follow the same notation as in previous sections for points that satisfy the LHC bounds, and denote by magenta squares those excluded. The points of category (ii) that cannot be tested, are drawn in gray. For clarity, we display only points corresponding to A-resonant channels (circles), higgsino DM (squares) and stop coannihilations (diamonds) which lie at high mass areas in which the non-tested models dominate; other classes of models lie in the same regions with the tested ones. The red solid boundary is obtained by combining the simplified model bounds from LHC searches. Since these models often do not apply to our particular cases, this boundary cannot be considered as an exclusion line (however, excluded points must be included in at least one of these contours). Nevertheless, it is useful to include this line for illustrative purposes, since it gives an idea of the range of masses explored at the LHC for every SUSY particle. For instance, the excluded points inside the red line of **Figure 3** are above the bound on electroweak searches through the multi-lepton + $\not{E}_T$ channel [56], the ones of **Figure 4** through strong production through the 0-lepton + jets + $\not{E}_T$ channel [57, 58], and the ones of **Figure 5** through the stop decays considered in ATLAS and CMS analyses [59–62].

As we have already emphasized, despite the fact that the left-right symmetric 4-2-2 unification differs from SO(10) by just one additional gaugino mass, this gives rise to novel possibilities for DM models. Even similar classes of models that satisfy

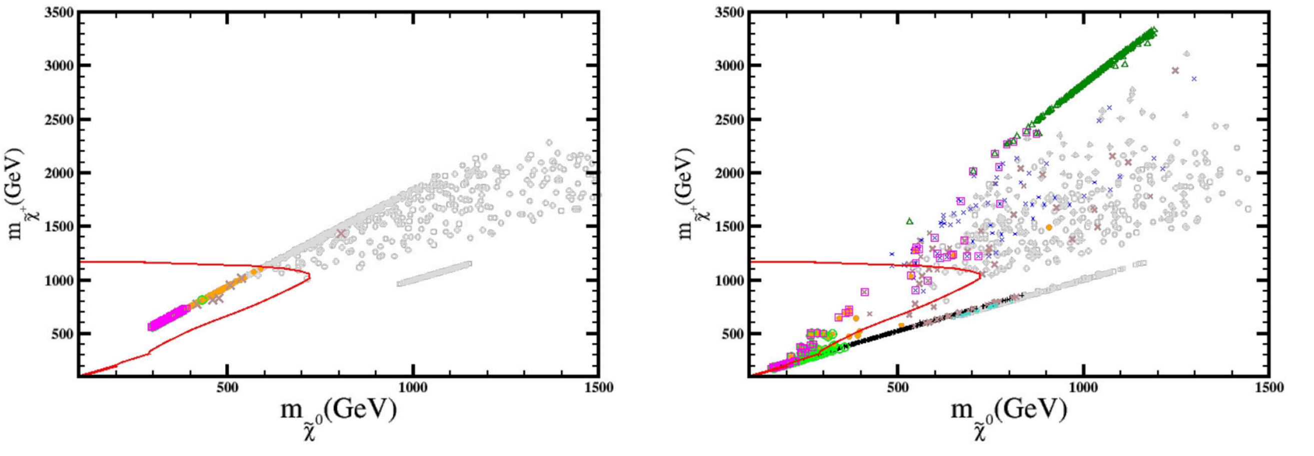

FIGURE 3 | Chargino masses vs. $m_{\tilde{\chi}^0}$ for the different models of SO(10) (left) and 4-2-2 (right). The points that can be compared with the LHC bounds follow the annotation of **Figure 1**, while the ones excluded are inside a purple square. Gray points correspond to models that cannot be decomposed to SMS LHC signals (circles for A-resonances, squares for higgsino DM and diamonds for stop coannihilations). The red line corresponds to the largest masses that LHC can probe, according to the CMS and ATLAS public analysis.

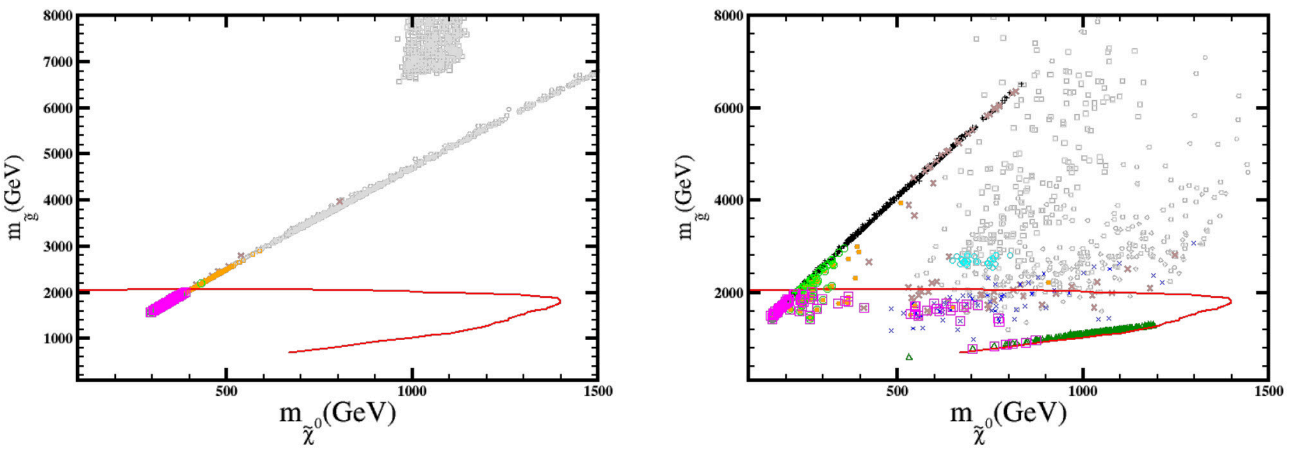

FIGURE 4 | As in **Figure 3** for the $m_{\tilde{g}}$ vs. m_{χ} scatter plot.

the DM constraints, now correspond to a different range of SUSY masses. This is due to the fact that the relic density constraints are satisfied through coannihilations, resonances or low values of the μ term, only in models with certain mass conditions (the areas of higgsino DM and A-resonances have larger values of SUSY partners in SO(10)). Consequently, the resulting LHC signals are very different in the two groups.

The SO(10) unified models are highly constrained by the LHC bounds. Most of the points that Smodels can compare with the LHC bounds are in the stau coannihilation area, and a good part of them are already excluded. These include a large majority of the models with a muon g-2 contribution at the $3-\sigma$ level. No points on the Higgsino DM region can be tested at the LHC according to the Smodels analysis and only a few points on the A-resonance area can be reached, none of them excluded by the current bounds. The excluded points are affected mostly by the gluino and stop bounds. We can see in **Figure 6** that the predicted sbottom masses are outside the LHC accessible area. The same happens with signals involving quarks of the lighter generations.

The 4-2-2 models have a richer structure with respect to experimental signatures at the LHC, than the ones arising from SO(10). In this case, we find points with higgsino DM and A-resonances in a wider spectrum of masses; moreover, we find a larger number of points that Smodels can decompose in signals that can be compared with the LHC bounds. In **Figure 3** we can see that models with chargino coannihilations have a compressed spectrum that results to light charginos compatible with the LHC bounds. However, we can see in **Figure 4** that such points are excluded by the gluino bounds. Despite that, some points predicting a relevant SUSY contribution to the muon g-2 are not yet excluded by the LHC. We can see in

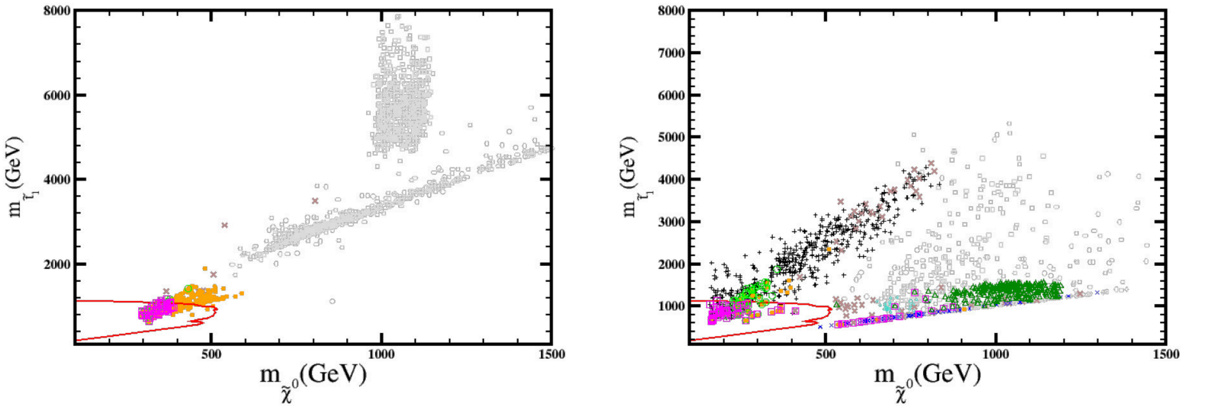

FIGURE 5 | As in **Figure 3** for the $m_{\tilde{t}}$ vs. $m_{\tilde{\chi}^0}$ scatter plot.

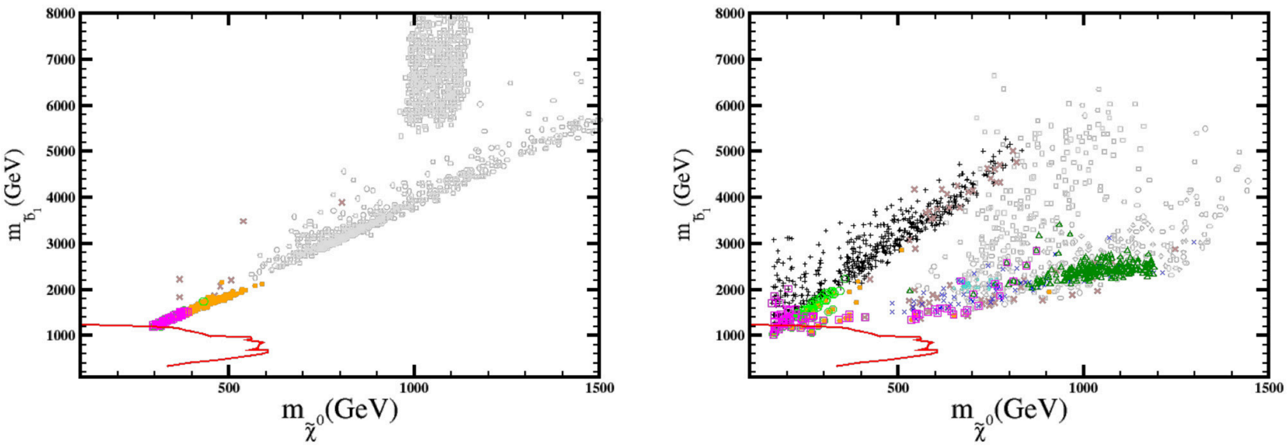

FIGURE 6 | As in **Figure 3** for the $m_{\tilde{b}}$ vs. $m_{\tilde{\chi}^0}$ scatter plot.

Figure 5 that bounds on stop searches affect many of the excluded points, while only a few models predict sbottom masses that can be affected by LHC. Processes involving first and second generation squarks are outside the scope of the current LHC bounds.

6. CONCLUSIONS

In this work we have performed a comparative study of $SO(10)$ and $SU(4)_c \times SU(2)_L \times SU(2)_R$ grand unification with respect to the LHC sparticle mass spectra, cold dark matter and muon $g-2$ predictions. Based on the remarkable complementarity between the LHC and dark matter searches, we show how the different patterns of soft SUSY-breaking terms at the GUT scale can be used to distinguish the two groups in experimental searches. Indeed, manifestation of specific features of the SUSY spectrum, either in DM searches or at the LHC, can be linked to different GUT symmetries, as discussed above.

In particular, the gauge and symmetry breaking structure of 4-2-2 enhances significantly the allowed parameter space as compared to SO(10), and gives rise to three additional coannihilation scenarios for dark matter (chargino, gluino and stop coannihilations). Even similar types of coannihilations that satisfy the DM constraints, now correspond to a different range of SUSY masses. Moreover, areas where the discrepancy between the theoretical and experimental values of muon g-2 can be reduced via a supersymmetric contribution are identified.

Gluino coannihilations are particularly important, since they are a unique feature of 4-2-2 and do not appear in other GUT schemes. They are a direct outcome of the particular gaugino mass relations of the model that results in relatively light gluinos. Chargino coannihilations are also found and, together with higgsino dark matter, are the most frequently encountered scenarios. Stop coannihilations also arise (these can also appear in flipped SU(5) [25]). In all cases, we get concrete predictions for the gaugino mass ratios that favor the respected scenarios and can be tested in future searches.

The overall message from the significant phenomenological differences between two groups that share so many common features is clear: although no SUSY signal has been found so far, there are still alternative possibilities to explore and the 4-2-2 group is one of them.

AUTHOR CONTRIBUTIONS

All authors listed have made a substantial, direct and intellectual contribution to the work, and approved it for publication.

ACKNOWLEDGMENTS

The research of MG was supported by the Spanish MINECO, under grants FPA2014-53631- C-2-P and FPA2017-86380-P. RR is supported by the Ramón y Cajal program of the Spanish MICINN, the Elusives European ITN project (H2020-MSCA-ITN-2015//674896- ELUSIVES), the SOM Sabor y origen de la Materia (PROMETEOII/2014/050) and Centro de excelencia Severo Ochoa Program under grant SEV-2014-0398. QS acknowledges support by the DOE grant No. DE-SC0013880.

REFERENCES

1. Aad G, Abajyan T, Abbott B, Abdallah J, Abdel Khalek S, Abdelalim AA, et al. Observation of a new particle in the search for the Standard Model Higgs boson with the ATLAS detector at the LHC. *Phys Lett B* (2012) **716**:1. doi: 10.1016/j.physletb.2012.08.020
2. Chatrchyan S, Khachatryan V, Sirunyan AM, Tumasyan A, Adam W, Aguilo E, et al. Observation of a new boson at a mass of 125 GeV with the CMS experiment at the LHC. *Phys Lett B* (2012) **716**:30. doi: 10.1016/j.physletb.2012.08.021
3. Akerib DS, Alsum S, Araújo HM, Bai X, Bailey AJ, Balajthy J, et al.. Results from a search for dark matter in the complete LUX exposure. *Phys Rev Lett.* (2017) **118**:021303. doi: 10.1103/PhysRevLett.118.021303
4. Akerib DS, Alsum S, Araújo HM, Arthurs M, Bai X, Bailey AJ, et al. Projected WIMP sensitivity of the LUX-ZEPLIN (LZ) dark matter experiment. *arXiv:1802.06039*.
5. Aprile E, Aalbers J, Agostini F, Alfonsi M, Amaro FD, Anthony M, et al. Physics reach of the XENON1T dark matter experiment. *J Cosmol Astropart Phys.* (2016) **1604**:027. doi: 10.1088/1475-7516/2016/04/027
6. Aprile E, Aalbers J, Agostini F, Alfonsi M, Amaro FD, Anthony M, et al. First dark matter search results from the XENON1T experiment. *Phys Rev Lett.* (2017) **119**:181301. doi: 10.1103/PhysRevLett.119.181301
7. Aalbers J, Agostini F, Alfonsi M, Amaro FD, Amsler C, Aprile E, et al. DARWIN: towards the ultimate dark matter detector. *J Cosmol Astropart Phys.* (2016) **1611**:017. doi: 10.1088/1475-7516/2016/11/017
8. Amole C, Ardid M, Arnquist IJ, Asner DM, Baxter D, Behnke E, et al. Dark matter search results from the PICO-60 C_3F_8 bubble chamber. *Phys Rev Lett.* (2017) **118**:251301. doi: 10.1103/PhysRevLett.118.251301
9. Komatsu E, Smith KM, Dunkley J, Bennett CL, Gold B, Hinshaw G, et al. Seven-Year Wilkinson microwave anisotropy probe (WMAP) observations: cosmological interpretation. *Astrophys J Suppl.* (2011) **192**:18. doi: 10.1088/0067-0049/192/2/18
10. Bennett CL, Larson D, Weiland JL, Jarosik N, Hinshaw G, Odegard N, et al. Nine-Year Wilkinson microwave anisotropy probe (WMAP) observations: final maps and results. *Astrophys J Suppl.* (2013) **208**:20. doi: 10.1088/0067-0049/208/2/20
11. Ade PAR, Aghanim N, Armitage-Caplan C, Arnaud M, Ashdown M, Atrio-Barandela F, et al. Planck 2013 results. XVI. cosmological Parameters. *Astron Astrophys.* (2014) **571**:A16. doi: 10.1051/0004-6361/201321591
12. Ade PAR, Aghanim N, Arnaud M, Ashdown M, Aumont J, Baccigalupi C, et al. Planck 2015 results. XIII. Cosmological parameters. *Astron Astrophys.* (2016) **594**:A13. doi: 10.1051/0004-6361/201525830
13. Goldberg H. Constraint on the photino mass from cosmology. *Phys Rev Lett.* (1983) **50**:1419. Erratum: [*Phys Rev Lett.* (2009) **103**:099905]. doi: 10.1103/PhysRevLett.103.099905
14. Ellis JR, Hagelin JS, Nanopoulos DV, Olive KA, Srednicki M. Supersymmetric relics from the big bang. *Nucl Phys B* (1984) **238**:453. doi: 10.1016/0550-3213(84)90461-9
15. Georgi H. The state of the art-gauge theories. *AIP ConfProc.* (1975) **23**:575–82. doi: 10.1063/1.2947450
16. Fritzsch H, Minkowski P. Unified interactions of leptons and hadrons. *Ann Phys.* (1975) **93**:193. doi: 10.1016/0003-4916(75)90211-0
17. Pati JC, Salam A. Lepton number as the fourth color. *Phys Rev D* (1974) **10**:275.
18. Mohapatra RN, Pati JC. Left-right gauge symmetry and an isoconjugate model of CP violation. *Phys Rev D* (1975) **11**:566. doi: 10.1103/PhysRevD.11.566
19. Senjanovic G, Mohapatra RN. Exact left-right symmetry and spontaneous violation of parity. *Phys Rev D* (1975) **12**:1502. doi: 10.1103/PhysRevD.12.1502
20. Magg M, Shafi Q, Wetterich C. Gauge hierarchy in presence of discrete symmetry. *Phys Lett.* (1979) **87B**:227. doi: 10.1016/0370-2693(79)90970-5
21. Lazarides G, Shafi Q. Comments on 'Monopole charges in unified gauge theories'. *Nucl Phys B* (1981) **189**:393.
22. Kibble TWB, Lazarides G, Shafi Q. Strings in SO(10). *Phys Lett.* (1982) **113B:**237. doi: 10.1016/0370-2693(82)90829-2
23. Lazarides G, Shafi Q. Superconducting membranes. *Phys Lett.* (1985) **159B:**261. doi: 10.1016/0370-2693(85)90246-1
24. Kibble TWB, Lazarides G, Shafi Q. Walls bounded by strings. *Phys Rev D* (1982) **26:**435. doi: 10.1103/PhysRevD.26.435
25. Cannoni M, Ellis J, Gómez ME, Lola S, Ruiz de Austri R. Supersymmetry searches in GUT models with non-universal scalar masses. *J Cosmol Astropart Phys.* (2016) **1603**:041. doi: 10.1088/1475-7516/2016/03/041
26. Okada N, Raza S, Shafi Q. Particle spectroscopy of supersymmetric SU(5) in light of 125 GeV higgs and muon g-2 data. *Phys Rev D* (2014) **90**:015020. doi: 10.1103/PhysRevD.90.015020
27. Dar S, Gogoladze I, Shafi Q, Un CS. Sparticle spectroscopy with neutralino dark matter from t-b-tau Quasi-Yukawa unification. *Phys Rev D* (2011) **84**:085015. doi: 10.1103/PhysRevD.84.085015
28. Kowalska K, Roszkowski L, Sessolo EM, Williams AJ. GUT-inspired SUSY and the muon g 2 anomaly: prospects for LHC 14 TeV. *J High Energy Phys.* (2015) **1506**:20. doi: 10.1007/JHEP06(2015)020
29. Kowalska K, Roszkowski L, Sessolo EM, Trojanowski S. Low fine tuning in the MSSM with higgsino dark matter and unification constraints. *J High Energy Phys.* (2014) **1404**:166. doi: 10.1007/JHEP04(2014)166
30. Ellis J, Evans JL, Mustafayev A, Nagata N, Olive KA. The super-GUT CMSSM revisited. *Eur Phys J C* (2016) **76**:592. doi: 10.1140/epjc/s10052-016-4437-6
31. Adeel Ajaib M, Li T, Shafi Q. LHC constraints on NLSP gluino and dark matter neutralino in yukawa unified models. *Phys Lett B* (2011) **705**:87. doi: 10.1016/j.physletb.2011.09.083
32. Raza S, Shafi Q, CS. NLSP gluino and NLSP stop scenarios from $b-\tau$ Yukawa unification. *Phys Rev D* (2015) **92**:055010. doi: 10.1103/PhysRevD.92.055010
33. Gogoladze I, Khalid R, Shafi Q. Yukawa unification and neutralino dark matter in SU(4)(c) x SU(2)(L) x SU(2)(R). *Phys Rev D* (2009) **79**:115004. doi: 10.1103/PhysRevD.79.115004
34. Gómez ME, Lola S, Ruiz De Austri R, Shafi Q. Dark matter, sparticle spectroscopy and muon $(g-2)$ in $SU(4)_c \times SU(2)_L \times SU(2)_R$. *JHEP* (2018) **2018**:62. doi: 10.1007/JHEP10(2018)062
35. Davier M, Hoecker A, Malaescu B, Zhang Z. Reevaluation of the hadronic contributions to the Muon g-2 and to alpha(MZ). *Eur Phys J C* (2011) **71**:1515. Erratum: [*Eur Phys J C* (2012) **72**:1874]. doi: 10.1140/epjc/s10052-012-1874-8
36. Allanach BC. SOFTSUSY: a program for calculating supersymmetric spectra. *Comput Phys Commun.* (2002) **143**:305. doi: 10.1016/S0010-4655(01)00460-X

37. Cerdeno DG, Gabrielli E, Gomez ME, Munoz C. Neutralino nucleon cross-section and charge and color breaking constraints. *J High Energy Phys.* (2003) **306**:30. doi: 10.1088/1126-6708/2003/06/030
38. Camargo-Molina JE, O'Leary B, Porod W, Staub F. Stability of the CMSSM against sfermion VEVs. *J High Energy Phys.* (2013) **1312**:103. doi: 10.1007/JHEP12(2013)103
39. Bertone G, Cerdeno DG, Fornasa M, Ruiz de Austri R, Strege C, Trotta R. Global fits of the cMSSM including the first LHC and XENON100 data. *J Cosmol Astropart Phys.* (2012) **1201**:15. doi: 10.1088/1475-7516/2012/01/015
40. Strege C, Bertone G, Feroz F, Fornasa M, Ruiz de Austri R, Trotta R. Global fits of the cMSSM and NUHM including the LHC Higgs discovery and new XENON100 constraints. *J Cosmol Astropart Phys.* (2013) **1304**:13. doi: 10.1088/1475-7516/2013/04/013
41. Bertone G, Calore F, Caron S, Ruiz R, Kim JS, Trotta R. Global analysis of the pMSSM in light of the Fermi GeV excess: prospects for the LHC Run-II and astroparticle experiments. *JCAP* (2016) **1604:**037. doi: 10.1088/1475-7516/2016/04/037
42. Belanger G, Boudjema F, Pukhov A, Semenov A. MicrOMEGAs 2.0: a Program to calculate the relic density of dark matter in a generic model. *Comput Phys Commun.* (2007) **176:**367. doi: 10.1016/j.cpc.2006.11.008
43. Gondolo P, Edsjo J, Ullio P, Bergstrom L, Schelke M, Baltz EA. DarkSUSY: computing supersymmetric dark matter properties numerically. *JCAP* (2004) **0407:**008. doi: 10.1088/1475-7516/2004/07/008
44. Mahmoudi F. SuperIso: a Program for calculating the isospin asymmetry of B —> K* gamma in the MSSM. *Comput Phys Commun.* (2008) **178**:745. doi: 10.1016/j.cpc.2007.12.006
45. Mahmoudi F. SuperIso v3.0, flavor physics observables calculations: Extension to NMSSM. *Comput Phys Commun.* (2009) **180**:1718. doi: 10.1016/j.cpc.2009.05.001
46. Savage C, Scaffidi A, White M, Williams AG. LUX likelihood and limits on spin-independent and spin-dependent WIMP couplings with LUXCalc. *Phys Rev D* (2015) **92**:103519. doi: 10.1103/PhysRevD.92.103519
47. Feroz F, Hobson MP. Multimodal nested sampling: an efficient and robust alternative to MCMC methods for astronomical data analysis. *Mon Not R Astron Soc.* (2008) **384:**449. doi: 10.1111/j.1365-2966.2007.12353.x
48. Feroz F, Hobson MP, Bridges M. MultiNest: an efficient and robust Bayesian inference tool for cosmology and particle physics. *Mon Not R Astron Soc.* (2009) **398**:1601. doi: 10.1111/j.1365-2966.2009.14548.x
49. Okawa H. Interpretations of SUSY searches in ATLAS with simplified models. arXiv:1110.0282
50. Chatrchyan S, Khachatryan V, Sirunyan AM, Tumasyan A, Adam W, Aguilo E, et al. Interpretation of searches for supersymmetry with simplified models. *Phys Rev D* (2013) **88**:052017. doi: 10.1103/PhysRevD.88.052017
51. Ambrogi F, Kraml S, Kulkarni S, Laa U, Lessa A, Magerl V, et al. SModelS v1.1 user manual: improving simplified model constraints with efficiency maps. *Comput Phys Commun.* (2018) **227**:72. doi: 10.1016/j.cpc.2018.02.007
52. Kraml S, Kulkarni S, Laa U, Lessa A, Magerl W, Proschofsky-Spindler D, et al. SModelS: a tool for interpreting simplified-model results from the LHC and its application to supersymmetry. *Eur Phys J C* (2014) **74**:2868. doi: 10.1140/epjc/s10052-014-2868-5
53. Ambrogi F, Kraml S, Kulkarni S, Laa U, Lessa A, Waltenberger W. On the coverage of the pMSSM by simplified model results. *Eur Phys J C* (2018) **78**:215. doi: 10.1140/epjc/s10052-018-5660-0
54. Djouadi A, Muhlleitner MM, Spira M. Decays of supersymmetric particles: the Program SUSY-HIT (SUspect-SdecaY-Hdecay-InTerface). *Acta Phys Polon B* (2007) **38**:635.
55. Sjstrand T, Ask S, Christiansen JR, Corke R, Desai N, Ilten P, et al. An introduction to PYTHIA 8.2. *Comput Phys Commun.* (2015) **191**:159. doi: 10.1016/j.cpc.2015.01.024
56. Sirunyan AM, Tumasyan A, Adam W, Ambrogi F, Asilar E, Bergauer T, et al. Combined search for electroweak production of charginos and neutralinos in proton-proton collisions at $\sqrt{s} = 13$ TeV. *J High Energy Phys.* (2018) **1803**:160. doi: 10.1007/JHEP03(2018)160
57. Sirunyan AM, Tumasyan A, Adam W, Ambrogi F, Asilar E, Bergauer T, et al. Search for supersymmetry in multijet events with missing transverse momentum in proton-proton collisions at 13 TeV. *Phys Rev D* (2017) **96**:32003. doi: 10.1103/PhysRevD.96.032003
58. Sirunyan AM, Tumasyan A, Adam W, Ambrogi F, Asilar E, Bergauer T, et al. Search for new phenomena with the M_{T2} variable in the all-hadronic final state produced in proton proton collisions at $\sqrt{s} = 13$ TeV. *Eur Phys J C* (2017) **77**:710. doi: 10.1140/epjc/s10052-017-5267-x
59. Aad G, Abbott B, Abdallah J, Abdel Khalek S, Abdinov O, Aben R, et al. Search for squarks and gluinos with the ATLAS detector in final states with jets and missing transverse momentum using $\sqrt{s} = 8$ TeV proton–proton collision data. *J High Energy Phys.* (2014) **1409**:176. doi: 10.1007/JHEP09(2014)176
60. Sirunyan AM, Tumasyan A, Adam W, Ambrogi F, Asilar E, Bergauer T, et al. Search for direct production of supersymmetric partners of the top quark in the all-jets final state in proton-proton collisions at $\sqrt{s} = 13$ TeV. *J High Energy Phys.* (2017) **1710**:5. doi: 10.1007/JHEP10(2017)005
61. Sirunyan AM, Tumasyan A, Adam W, Ambrogi F, Asilar E, Bergauer T, et al. Search for supersymmetry in proton-proton collisions at 13 TeV using identified top quarks. *Phys Rev D* (2018) **97**:012007. doi: 10.1103/PhysRevD.97.012007
62. Sirunyan AM, Tumasyan A, Adam W, Ambrogi F, Asilar E, Bergauer T, et al. Search for top squark pair production in pp collisions at $\sqrt{s} =$ 13 TeV using single lepton events. *J High Energy Phys.* (2017) **1710**:19. doi: 10.1007/JHEP10(2017)019

Conflict of Interest Statement: The authors declare that the research was conducted in the absence of any commercial or financial relationships that could be construed as a potential conflict of interest.